0970290, 2023, 1, Downlo

ibary.viley.com/doi/10.1002/bit.28249 by University Of Mimeson Lib, Wiley Online Library on [26/02/2023]. See the Terms and Conditions (https://onlinelibary.wiley.com/terms-and-conditions) on Wiley Online Library for rules of use; OA articles are governed by the applicable Creative Commons

ARTICLE



Kinetic-model-based pathway optimization with application to reverse glycolysis in mammalian cells

Yen-An Lu¹ | Conor M. O' Brien¹ | Douglas G. Mashek² | Wei-Shou Hu¹ | Qi Zhang¹

Correspondence

Qi Zhang and Wei-Shou Hu, 421 Washington Ave SE, Minneapolis, MN 55455-0132 USA. Email: qizh@umn.edu and wshu@umn.edu

Funding information

National Science Foundation

Abstract

Over the last two decades, model-based metabolic pathway optimization tools have been developed for the design of microorganisms to produce desired metabolites. However, few have considered more complex cellular systems such as mammalian cells, which requires the use of nonlinear kinetic models to capture the effects of concentration changes and cross-regulatory interactions. In this study, we develop a new two-stage pathway optimization framework based on kinetic models that incorporate detailed kinetics and regulation information. In Stage 1, a set of optimization problems are solved to identify and rank the enzymes that contribute the most to achieving the metabolic objective. Stage 2 then determines the optimal enzyme interventions for specified desired numbers of enzyme adjustments. It also incorporates multi-scenario optimization, which allows the simultaneous consideration of multiple physiological conditions. We apply the proposed framework to find enzyme adjustments that enable a reverse glucose flow in cultured mammalian cells, thereby eliminating the need for glucose feed in the late culture stage and enhancing process robustness. The computational results demonstrate the efficacy of the proposed approach; it not only captures the important regulations and key enzymes for reverse glycolysis but also identifies differences and commonalities in the metabolic requirements for different carbon sources.

KEYWORDS

gluconeogenesis, glucose metabolism, kinetic model, metabolic model, optimization, pathway engineering

1 | INTRODUCTION

For decades, metabolic engineering has been successfully used to rewire metabolism to produce desired metabolites (Huccetogullari et al., 2019; Lian et al., 2018; Liu & Nielsen, 2019). While much of the effort has been guided by physiological knowledge, there has been an increasing number of approaches that use metabolic models and mathematical optimization to aid the pathway design process. In model-based pathway optimization, the optimization problem is defined by a metabolic objective, such as maximizing the production

rate of a specific metabolite, an underlying metabolic model, physical restrictions in the form of inequality constraints, and a set of enzymes that can be adjusted to achieve the given metabolic objective. Powerful optimization algorithms can then be used to find the optimal enzyme adjustments without exhaustively exploring the entire search space (Chae et al., 2017; Machado & Herrgård, 2015; Zomorrodi et al., 2012).

The metabolic model is the center piece of any model-based pathway optimization method. While its scope can range from focusing on only a few pathways to encompassing reactions at

¹Department of Chemical Engineering and Materials Science, University of Minnesota, Minneapolis, Minnesota, USA

²Department of Biochemistry, Molecular Biology and Biophysics, University of Minnesota, Minneapolis, Minnesota, USA

genome scales (Edwards & Palsson, 2000; Monk et al., 2017), it generally consists of mass balance equations for substrates and metabolites. The rate of each reaction can be represented as a physical quantity of flux or expressed as a function of the concentrations of the relevant substrates and allosteric regulators, leading to a stoichiometric or a kinetic model, respectively. Most existing pathway optimization tools use stoichiometric models and have mainly been applied to microorganisms, where the goal is to achieve overproduction of desired biochemicals (Lin et al., 2017; Yim et al., 2011). Different genetic interventions have been considered, including gene knockout (Burgard & Maranas, 2003), gene knock-in as well as up/downregulation (Kim et al., 2011; Pharkya et al., 2004), and perturbations of transcriptional regulatory networks (Shen et al., 2019).

Kinetic metabolic models are required when it is important to capture the effect of enzyme and metabolite concentrations as well as allosteric regulations at the pathway and system levels (Foster et al., 2021). This is true in the case of tissue cells of higher organisms, especially mammals. Because of their capability in many posttranslational modifications, mammalian cells are the major workhorse for the biomanufacturing of therapeutic proteins for which the manipulation of pathways, especially those of energy metabolism (EM), can greatly impact the process outcome (Mulukutla et al., 2010; Richelle & Lewis, 2017; Templeton & Young, 2018). However, the complex regulations make the kinetic models highly nonlinear. In addition, in pathway optimization, binary variables are commonly used to indicate which enzymes are chosen to be adjusted: in combination with the nonlinear kinetic models, this results in optimization problems in the form of mixed-integer nonlinear programs (MINLPs), which are notoriously difficult to solve. It is due to this computational complexity (and often the difficulty of building an accurate kinetic metabolic model in the first place) that pathway optimization using kinetic models has rarely been applied in the literature.

There are various methods that employ some form of local sensitivity analysis of kinetic models to guide pathway design, but they cannot guarantee optimality and are restricted to small perturbations (Kacser et al., 1995; Moreno-Sánchez et al., 2008). A few attempts have been made to directly solve the MINLP pathway optimization problem, but they are confined to simplified systems without detailed regulation (Nikolaev, 2010; Polisetty et al., 2008; Villaverde et al., 2016). Other approaches try to avoid the computational challenge of solving an MINLP by applying a linear approximation of the kinetic model, which results in a much easier mixed-integer linear program (MILP) (Hatzimanikatis et al., 1996; Vera et al., 2010). However, these approaches do not apply to large metabolic changes (Vital-lopez et al., 2006). Other studies have focused on hybrid methods that combine stoichiometric and kinetic models; for example, k-OptForce solves a stoichiometric model with a subgroup of reactions that have kinetic information to identify enzyme interventions (Chowdhury et al., 2014).

A recent work introduced an optimization framework that avoids binary variables by incorporating convex penalty terms, resulting in a nonlinear programming (NLP) problem (Lucidi & Rinaldi, 2010, 2013; O'Brien et al., 2019). Using the kinetic model of Mulukutla et al. (Mulukutla et al., 2014, 2015), the optimization framework was applied to identify target enzymes to be subjected to modifications to mitigate the Warburg effect. However, the framework requires the generation of a large number of initial guesses to determine a set of local optima, which affects its efficacy to identify optimal interventions on a multi-target basis and yet still does not guarantee global optimality.

In this study, we propose an efficient optimization framework that integrates kinetic metabolic models to identify the optimal multi-enzyme interventions for specified engineering goals. Implementing the convex penalty method, a new two-stage strategy is proposed, where Stage 1 identifies the enzymes that have high impacts on achieving the metabolic objective and Stage 2 determines the optimal enzyme interventions for specified numbers of enzyme adjustments. The optimization problem is formulated to consider both gene insertion as well as up/downregulation. To avoid the generation of large sets of local optima, the problem is solved using a state-of-the-art global optimization solver. Moreover, multi-scenario optimization is implemented to simultaneously target multiple physiological conditions.

Using a developed kinetic EM model of proliferating mammalian cells, we apply the proposed framework to identify the optimal enzyme interventions to reverse the flux direction of glycolysis from various substrates. Glucose is the main substrate of mammalian cells in culture. During the growth phase, cells can wastefully convert the vast majority of glucose to lactate which accumulates to inhibit growth, a phenomenon also seen in cancer cells and called the Warburg effect (Buchsteiner et al., 2018; Hassell et al., 1991; Lao & Toth, 1997). While cells in culture can switch from Warburg type of glycolysis to lactate consumption, which was shown to be associated with higher productivity (Charaniya et al., 2010), glucose consumption continues albeit at a lower rate (Mulukutla et al. 2012, 2015). This is attributed to the inability of cells to reverse the carbon flow in glycolysis to generate glucose for synthesizing NADPH, ribulose-5phosphate as well as glycans. However, unmanaged glucose feeding causes glucose accumulation and potentially results in a return to lactate production (Gagnon et al., 2011). Hence, empowering cells to synthesize glucose while under metabolic shift would eliminate the need of supplying glucose, potentially increasing process robustness. Applying the proposed method, we conducted computational case studies targeting different carbon source scenarios. We were able to identify the optimal adjustments in enzyme levels and metabolite concentrations, which align with the physiological understanding of reverse glycolysis.

2 | METHODS

2.1 | Kinetic model

A previously developed kinetic model of energy metabolism of proliferating mammalian cells is used in this study (Mulukutla

10970290, 2023, 1, Downloaded from https://onlinelibrary.wiley.com/doi/10.1002/bit.28249 by University Of Mimesota Lib, Wiley Online Library on [26/02/2023]. See the Terms

on Wiley Online Library for rules of use; OA articles are governed by the applicable Creative Common

et al., 2015). An overview of the metabolic network is given in Figure 1. Since we focus on metabolic changes under fixed extracellular conditions, a steady-state assumption is applied. Pivotal allosteric regulations considered include fructose-1,6-bisphosphate (F16BP) activations of phosphofructokinase (PFK) and pyruvate kinase (PK), fructose-2,6-bisphosphate (F26BP) modulation of PFK, phosphoenolpyruvate (PEP) activation of 6phosphofructo2kinase/ fructose2,6bisphosphatase (PFKFB), and lactate inhibition of PFK. To enable a reverse glycolytic flux, we also include additional gluconeogenic (GNG) enzymes: glucose-6-phosphatase (G6Pase),

fructose-1,6-bisphosphatase 1 (FBP1), pyruvate carboxylase (PC), and both the cytosolic and mitochondrial isoforms of phosphoenolpyruvate carboxykinase (PCK1 and PCK2). Since the main metabolites of the pentose phosphate pathway (PPP), for example, NADPH and phosphosugars, do not participate in the reactions of gluconeogenesis, PPP is not considered in the model. The mitochondrial phosphoenolpyruvate transporter (PEPx) is included to export the PEP generated by PCK2 into the cytosol. The six GNG enzymes constitute the enzyme (reaction) set \mathscr{R}^{GNG} while the original enzymes of the model form the set \mathcal{R}^{EM} . The detailed kinetic

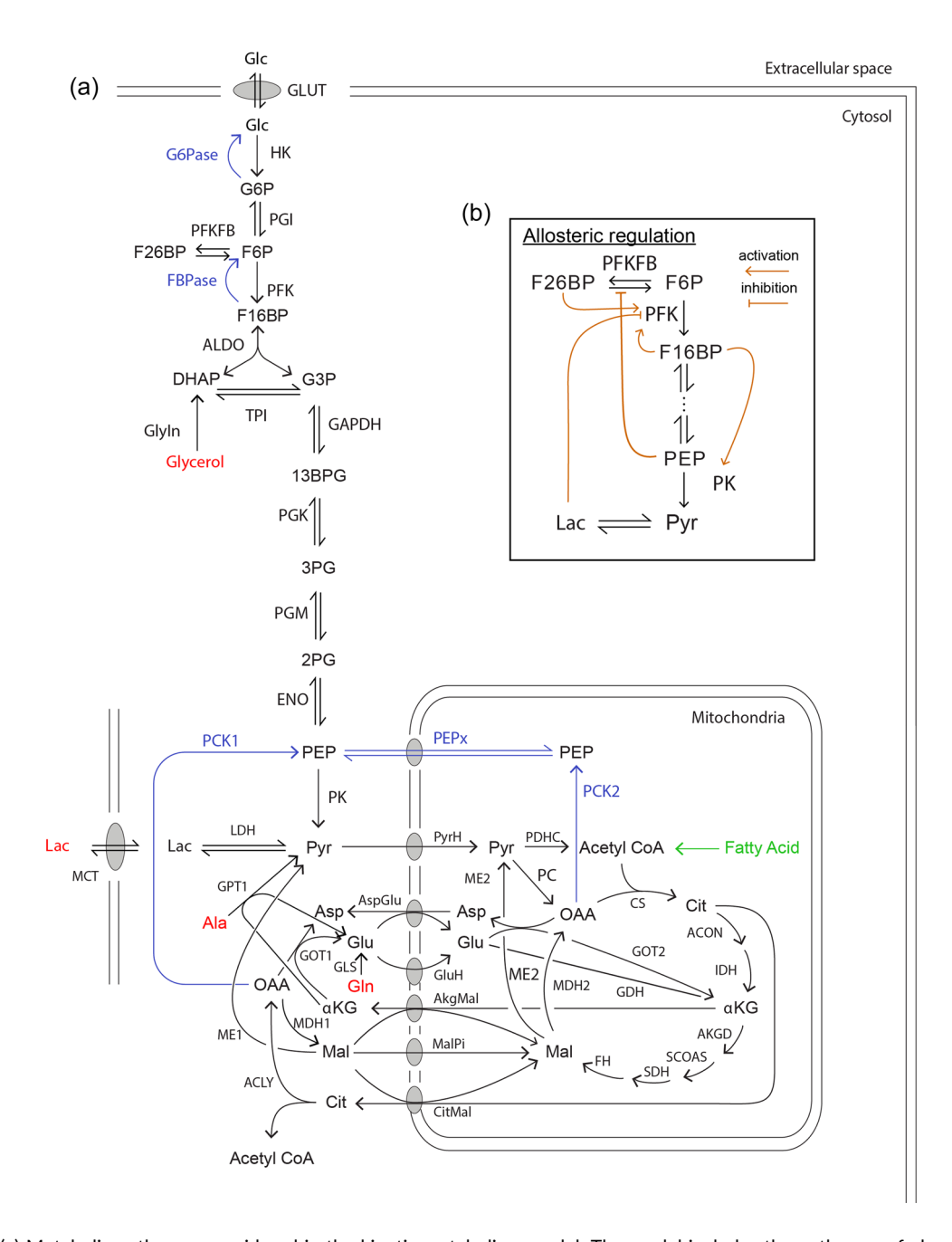


FIGURE 1 (a) Metabolic pathways considered in the kinetic metabolism model. The model includes the pathways of glycolysis, gluconeogenesis, TCA cycle, and malate-aspartate shuttles. Four substrates of gluconeogenesis are considered: lactate, alanine, glutamine, and glycerol (red). Enzyme sets are divided into two sets, \mathscr{R}^{EM} and \mathscr{R}^{GNG} , shown in black and blue, respectively. An extra energy supply from fatty acid breakdown is considered, shown in green. (b) Pivotal allosteric regulation of glycolysis considered.

BIOTECHNOLOGY BIOENGINEERING WILEY 219

$$1 \le \alpha_i \le \alpha_i^{max} \quad \forall j \in \mathcal{R}^{GNG}$$
 (1f)

$$g(\alpha, r, C) \ge 0.$$
 (1g)

equations and parameters of \mathscr{R}^{EM} can be found in our previous publication (Mulukutla et al., 2015). Reaction equations and parameters of \mathscr{R}^{GNG} are collected from liver models (Berndt et al., 2018; König et al., 2012). The bifunctional enzyme PFKFB in \mathscr{R}^{EM} is a major flux regulator through its varying ratio of kinase/phosphatase activity, where its kinase activity phosphorylates fructose-6-phosphate (F6P) to fructose2,6bisphosphate (F26BP), and the phosphatase activity hydrolyzes F26BP back to F6P (Rider et al., 2004; Wu et al., 2001). A parameter σ is introduced to denote this ratio.

Among the four carbon sources considered, lactate (Lac) enters the pathway network through lactate dehydrogenase A (LDHA) which is already included in the kinetic model. Additionally, alanine transaminase 1 (GPT1) and glutaminase (GLS) are considered for alanine (Ala) and glutamine (Gln), respectively. The uptake of glycerol (Glyc) is catalyzed by a series of reactions converting glycerol to dihydroxyacetone phosphate (DHAP) and is represented by GlyIn. Each of the corresponding fluxes, r_{LDHA} , r_{GPT1} , r_{GLS} , and r_{GlyIn} , is set to zero when the compound is not the carbon source being considered. To represent the reverse glycolysis, the extracellular glucose concentration is set to 5 mM, and the substrate concentrations of Lac, Ala, and Gln are set to be 2, 1, and 1 mM, respectively. Moreover, since gluconeogenesis is an endothermic pathway, the energy source is supplied from the mitochondria acetyl-CoA (mAcCoA) input from β -oxidation of fatty acids, denoted by r_{fox} .

2.2 | Mathematical formulation of optimization problems

Optimization problems are formulated to identify the minimum adjustments in enzyme abundance that maximize a specific pathway engineering goal. Two different types of optimization problems are proposed: single-scenario optimization (SSO), which generally considers one specific set of physiological conditions, and multi-scenario optimization (MSO), which simultaneously considers multiple sets of physiological conditions, each represented by one scenario.

2.2.1 | Single-scenario optimization

The SSO problem can be generally formulated as follows:

(SSO) : minimize
$$r_{\text{GLUT}} + \lambda \sum_{j \in \mathscr{R}} (\log_{10} \alpha_j)^2$$
 (1a)

subject to
$$\sum_{i \in \mathcal{R}_i} w_{ij} r_j = 0 \quad \forall i \in \mathcal{M}$$
 (1b)

$$r_j = f\left(\alpha_j \cdot E_j, k_j^{\text{cat}}, K_j, C_j\right) \quad \forall j \in \mathcal{R}^{\text{EM}}$$
 (1c)

$$r_j = f\left((\alpha_j - 1) \cdot E_j, k_j^{\text{cat}}, K_j, C_j\right) \quad \forall j \in \mathscr{R}^{\text{GNG}}$$
 (1d)

$$\alpha_i^{\min} \le \alpha_i \le \alpha_i^{\max} \quad \forall \ j \in \mathcal{R}^{\mathsf{EM}}$$
 (1e)

The notation is such that boldface letters denote vectors while scalar quantities are denoted by non-boldface letters. The reaction (enzyme) set of the targeted metabolic network is denoted by \mathcal{R} , where $\mathcal{R} = \mathcal{R}^{EM} \cup \mathcal{R}^{GNG}$. The relative change in the abundance level of enzyme $j \in \mathcal{R}$ is denoted by α_i . An additional α_{σ} is assigned to σ to capture the impact of the change in the activity ratio of kinase/phosphatase in PFKFB. Since a negative r_{GLUT} value represents glucose production, minimizing r_{GLUT} is selected as the metabolic objective, as indicated by the first term of the objective function (1a). The second term of (1a) penalizes the sum of squared logarithms of α_i over the set \mathscr{R} with a weighting factor λ , which is modulated to find a good trade-off between the metabolic objective and the magnitude of enzyme level adjustments. A squared logarithm of α_i is chosen to ensure that no penalty is applied if the enzyme level is not changed ($\alpha_i = 1$), and that the same magnitudes of downregulation and upregulation of enzyme abundance are penalized equally. Constraints (1b)-(1d) correspond to the kinetic mechanistic model of the targeted metabolic network at steady state. Equations (1b) represent the material balance of each metabolite $i \in \mathcal{M}$, where *M* denotes the set of metabolites, considering the reaction stoichiometry with wij denoting the stoichiometric coefficient of metabolite *i* in reaction *j*; \mathcal{R}_i denotes the set of reactions that involve metabolite i. Equations (1c) and (1d) model the kinetics of each reaction j in \mathscr{R}^{EM} and \mathscr{R}^{GNG} , respectively. Each reaction rate r_i is a function of α_i , the original enzyme level E_i , the catalytic constant k_i^{cat} , a set of kinetic parameters K_i , and a set of concentrations C_j . In Equation (1d), 1 is subtracted from α_j to ensure that the new reaction is not considered when α_i is equal to 1, which represents the original state of the targeted network. Constraints (1e) and (1f) define the lower bounds (α_i^{\min}) and upper bounds (α_i^{\max}) on α_i , where the lower bounds of enzymes in \mathscr{R}^{GNG} are set to 1, which is equivalent to no expression of the corresponding enzyme. Constraints (1g) compactly represent additional biological constraints that specify bounds on metabolite concentrations and metabolic fluxes, ATP and NADH flux balances, and constraints on substrates as well as energy supplies. Detailed descriptions of (1g) are included in the supplementary information.

2.2.2 | Multi-scenario optimization

When SSO is performed, only one specific carbon source, i.e. Lac, Ala, Gln, or Glyc, is considered. This can be a significant limitation if we want to engineer a metabolic system that can effectively use all four carbon sources to produce glucose since the optimal enzyme adjustments for one carbon source may not perform well for another. Hence, to simultaneously consider all four carbon sources, we propose to solve the following MSO problem:

(MSO): minimize
$$\sum_{\alpha, r_s, C_s} r_{s,GLUT} + \lambda \sum_{i \in \mathscr{R}} (\log_{10} \alpha_i)^2$$
 (2a)

subject to
$$\sum_{i \in \mathcal{X}_{i}} w_{ij} r_{sj} = 0 \quad \forall \ i \in \mathcal{M}, \forall \ s \in \mathcal{S}$$
 (2b)

$$r_{sj} = f\left(\alpha_j \cdot E_j, k_j^{cat}, \textbf{\textit{K}}_j, \textbf{\textit{C}}_{sj}\right) \quad \forall \ j \in \mathscr{R}^{\text{EM}}, \forall \ s \in \mathscr{S} \tag{2c}$$

$$r_{sj} = f\left((\alpha_j - 1) \cdot E_j, k_j^{cat}, \mathbf{K_j}, \mathbf{C_{sj}}\right) \quad \forall j \in \mathcal{R}^{GNG}, \forall s \in \mathcal{S}$$
 (2d)

$$\alpha_i^{min} \le \alpha_i \le \alpha_i^{max} \quad \forall \ j \in \mathcal{R}^{EM}$$
 (2e)

$$1 \le \alpha_i \le \alpha_i^{max} \quad \forall \ j \in \mathcal{R}^{GNG}$$
 (2f)

$$g_s(\boldsymbol{\alpha}, \mathbf{r}_s, \mathbf{C}_s) \ge 0 \quad \forall \ s \in \mathcal{S},$$
 (2g)

where \mathscr{S} denotes the set of scenarios, with each scenario generally representing a different set of conditions imposed on the system, as reflected in (2g) where the constraints $g_s(\cdot) \geq 0$ can be different for each scenario s. In our particular case, each scenario s corresponds to a specific carbon source. The goal of MSO is to determine a common set of changes in enzyme abundance levels that maximize the sum of reverse glycolysis flux across all four scenarios. As such, the same variables \mathfrak{a} apply to all scenarios whereas the reaction rates r_s and metabolite concentrations \mathbf{C}_s can vary across scenarios, hence the added scenario index s. Note that the same metabolic model is applied to all scenarios, as indicated by Equations (2b)–(2d).

2.3 | Two-stage optimization framework

A two-stage optimization framework, which applies to both SSO and MSO, is proposed to first identify a subset of enzymes whose abundance changes can significantly improve the targeted metabolic goal and subsequently identify the best enzyme interventions while limiting the number of enzymes that can be perturbed. The latter step is important since, in practice, one would like to minimize the number of enzymes that need to be altered to satisfy the metabolic objective. An overview of the proposed algorithm in the form of a flowchart is shown in Figure 2.

2.3.1 | Stage 1: Identifying key enzymes

When the pathway optimization problem, i.e. (SSO) or (MSO), is solved in Stage 1, we allow all enzymes to change. However, we seek to find the subset of enzymes that contribute the most to achieving the metabolic objective, and we do so by varying the value of the penalty parameter λ , which indirectly controls to what extent the enzymes should be altered. The desired set of key enzymes is obtained at a specific λ value, which we typically choose to be the largest λ that achieves the optimal metabolic objective value. The key enzyme set, denoted by $\mathscr{R}^{\text{stg1}}$, is identified by selecting the enzymes for which the optimal α_i satisfies the following criterion:

$$(\log_{10} \alpha_j)^2 \geq \delta, \tag{3}$$

where δ denotes the cutoff threshold.

2.3.2 | Stage 2: Determining optimal interventions for fixed numbers of enzyme adjustments

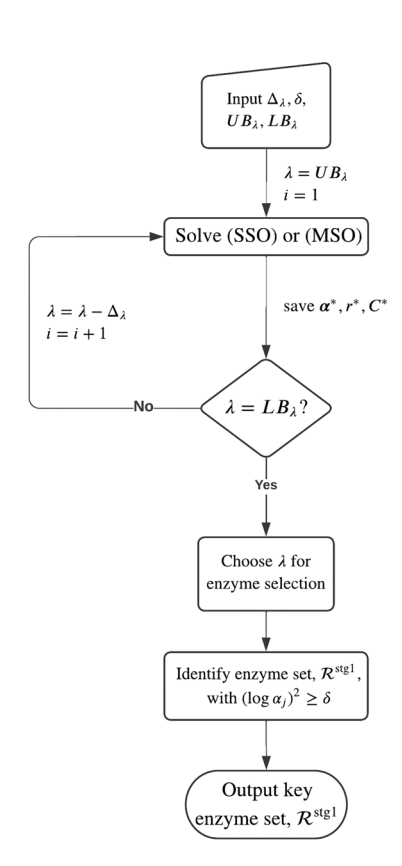
In Stage 2, as illustrated in Figure 2, all possible combinations of enzymes from the enzyme set $\Re^{\operatorname{stg1}} \backslash \Re^{\operatorname{ex}}$ are generated for different specified numbers of enzymes. Typically, we start with the number of enzyme adjustments n=1 and increase it after each iteration until the maximum desired number N is reached. We refer to \Re^{ex} as the exclusive enzyme set, which contains the enzymes that are always allowed to change in the Stage-2 optimization. In this study, GNG and carbon-entry enzymes are included in \Re^{ex} . SSO or MSO is then performed for each combination of enzymes by allowing only the abundance levels of those enzymes and the ones in \Re^{ex} to change while keeping other enzymes at their original abundance levels. Optimal solutions of all enzyme combinations and the corresponding enzyme interventions are collected and compared to identify the optimal enzyme adjustments.

2.4 | Implementation details

The algorithms were implemented in Python 3.7, where the optimization problems were modeled using the modeling language Pyomo (Hart et al., 2017). All model instances were solved using the global solver BARON (Sahinidis, 1996) with CPLEX as the linear programming (LP) subsolver and IPOPT as the NLP subsolver (Andreas & Lorenz, 2006). All computations were performed on AMD EPYC 7702 processors using resources from the Minnesota Supercomputing Institute.

3 | RESULTS AND DISCUSSION

The reverse of glycolysis, i.e. gluconeogenesis, takes place in the liver and kidney of mammals. It requires adjustments in the expressions of enzymes not only to overcome the four irreversible reactions in glycolysis but also to alter the concentrations of many intermediate metabolites and regulators in the cytosol and mitochondrion. It should be noted that cultured cells express the enzyme isoforms typically seen in proliferating cells exhibiting the Warburg effect, but not the liver isoforms. Reversing its flow may be more complex than in gluconeogenic tissues. We applied the proposed framework to determine the optimal enzyme adjustments to reverse the glucose flow in proliferating mammalian cells. Using SSO and MSO, two computational case studies were performed to identify the differences and commonalities in the metabolic requirements for reversing glycolysis with various carbon sources.



Stage 2: determining optimal interventions for fixed numbers of enzyme adjustments

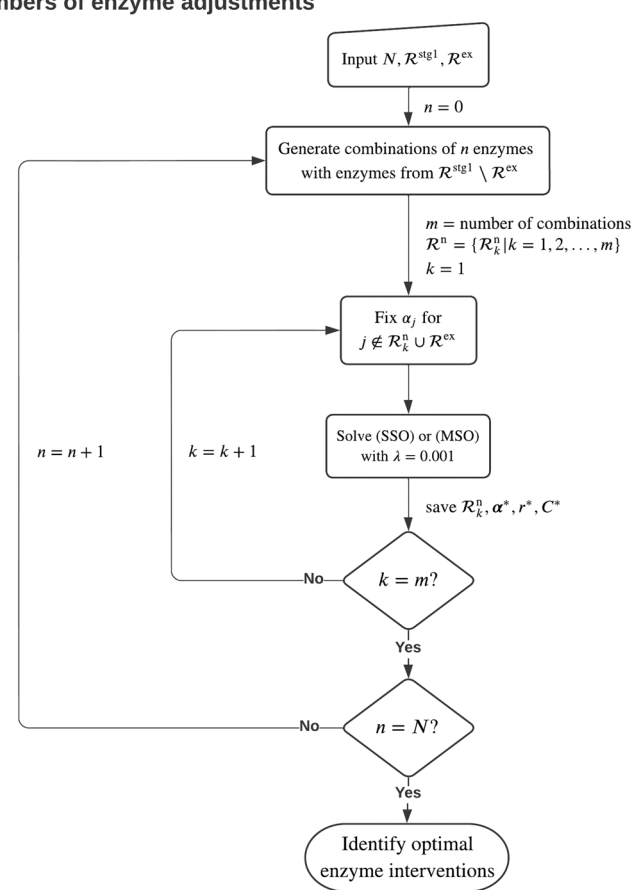


FIGURE 2 Flowchart of the two-stage optimization framework. Stage 1: All-enzyme SSO or MSO is performed for a defined range of penalty weight values λ (defined by the upper and lower bounds UB_{λ} and LB_{λ}) to identify the key enzyme set $\mathcal{B}^{\text{stg1}}$, where Δ_{λ} denotes the step size when changing λ , and δ is the threshold value selected for the identification of the key enzyme set. Stage 2: Combinations of n enzymes are generated from the enzyme set $\mathscr{R}^{stg1}/\mathscr{R}^{ex}$ to form the enzyme sets \mathscr{R}^{n}_{k} . The exclusive enzyme set \mathcal{R}^{ex} includes the enzymes that are always allowed to change in Stage-2 optimization. SSO or MSO is performed with different combinations of enzymes allowed to change to identify the best interventions for all n = 1, ..., N, where N is the maximum desired number of enzyme adjustments.

Case study 1: Reversing glucose flow using different carbon sources

We consider four different substrates, Lac, Ala, Glu, and Glyc. All four are naturally used for gluconeogenesis in the liver and kidney of mammals or readily supplied in the cell culture medium. Lactate is the major metabolite produced during cell growth. Alanine is also frequently excreted in the culture medium. Glutamine is typically supplied as a nutrient at a high level. Glycerol derived from lipid catabolism is an important carbon source for gluconeogenesis. SSO is first performed to test if the addition of the GNG enzymes alone is sufficient to reverse the glucose flow. To do so, we set the penalty weight λ in the objective function of (SSO) to a very small value (10⁻⁵); note that we could have set it to zero but did not do so for numerical reasons. The upper bounds of α_i for $j \in \mathcal{R}^{EM} \cup \mathcal{R}^{GNG}$ are set to 100, and the lower bounds of α_i for $j \in \mathcal{R}^{EM}$ are set to 0.01.

As shown in Table 1, by solely expressing the GNG enzymes and fixing the EM enzymes at their original levels, low or no glucose production is obtained in all four scenarios. In contrast, high glucose production rates are achieved when all enzymes in $\mathscr{R}^{\mathrm{EM}}$ and $\mathscr{R}^{\mathrm{GNG}}$ are allowed to change in their abundance levels. To identify the optimal enzyme combinations as well as adjustments in \mathcal{R}^{EM} for different fixed numbers of altered enzymes, the proposed two-stage framework is applied.

3.1.1 Stage-1 results

Identification of the optimal enzyme interventions in $\mathscr{R}^{\mathsf{EM}}$ for a fixed number of enzyme adjustments can be approached by exhaustively listing all possible enzyme combinations across $\mathscr{R}^{\mathsf{EM}}$ and solving the corresponding optimization problems. However, due to the large cardinality of \mathcal{R}^{EM} , the number of optimization

10970290, 2023, 1, Downloaded

from https://onlinelibrary.wiley.com/doi/10.1002/bit.28249 by University Of Minnesota Lib, Wiley Online Library on [26/02/2023]. See the Terms

on Wiley Online Library for rules of use; OA articles are governed by the applicable Creative Common

instances to be solved would be very large even for a moderate number of enzyme adjustments. Stage 1 aims to reduce the number of candidate enzymes that need to be considered. This is achieved by increasing the penalty on enzyme adjustments, i.e. a higher λ value, which decreases the incentive to change the abundance of enzymes that do not significantly improve the metabolic objective, i.e. reverse glycolysis flux. In other words, an appropriate selection of λ can result in a reasonably small set of key enzymes, $\mathscr{R}^{\text{stg1}}$, whose changes in abundance most meaningfully contribute to glucose synthesis.

(SSO) is solved with different values of λ over six orders of magnitude (10^{-3} – 10^{3}) for each of the carbon source scenarios, as shown in Figure 3a. For each carbon source, glucose production increases with decreasing λ and reaches a constant minimum r_{GLUT} for sufficiently small λ values. The cut-off threshold δ for enzyme selection is set to 0.03, which is approximately a 1.5-fold increase/decrease in the enzyme levels. Using the GIn

TABLE 1 Optimized glucose flux, r_{GLUT} in each carbon source scenario with SSO subjected to different sets of enzymes that are allowed to change in their abundance levels

	Optimal r _{GLUT}	[mM/h]
Scenario	$_{\mathscr{R}}$ GNG	$\mathscr{R}^{EM} \cup \mathscr{R}^{GNG}$
Lac	-0.3	-25
Ala	9.9	-16.7
Gln	0.0	-25
Glyc	-0.1	-25

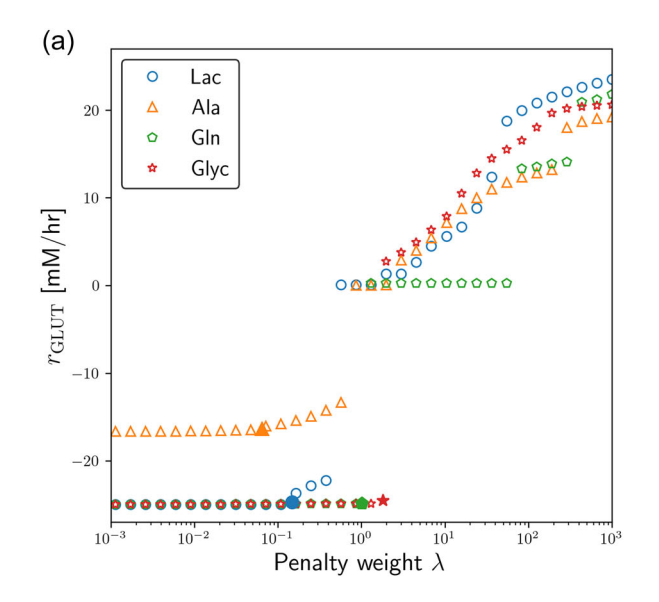
Note: Negative flux indicates glucose production. The penalty weight is set to 10^{-5} due to numerical reasons.

scenario as an example, Figure 3b shows that the number of selected enzymes increases with decreasing λ . \mathscr{R}^{stg1} is defined at the λ value that represents a trade-off between the improvement in glucose production and the minimization of the number of enzyme adjustments. The size of \mathscr{R}^{stg1} is 10, significantly lower than the cardinality of \mathscr{R}^{EM} of 41. Similar reductions in the number of selected enzymes are observed in the other carbon source scenarios, as shown in Figure S1.

The key EM enzymes, along with their α_j values, grouped by different pathways are shown in Figure S2. Common to all four scenarios is the amplification of entry enzymes. Glycerol is a special case as it enters directly the upper glycolysis pathway and requires only a few key enzyme changes. For the other three carbon sources, HK is suppressed to reduce the glycolysis flux. TCA cycle enzyme changes are more diverse for the three carbon sources as each enters the TCA cycle at different points and each has a different route for channeling PEP into reversed glycolysis. It should be noted that the selection of bounds on α affects the key enzyme selection, where a smaller bound constrains the reverse glucose flow, as shown in Figure S3. To eliminate the impact of α bounds on enzyme selection, we choose 100 fold-change as the selected bounds in this study.

3.1.2 | Stage-2 results

Stage-2 optimization is performed to identify the optimal enzyme interventions for different numbers of allowed enzyme adjustments. Aside from the GNG enzymes, carbon-entry enzymes are allowed to vary in their abundance so as not to limit the supply of substrates. In addition, combinations of up to five enzymes from \Re^{stg1} are allowed



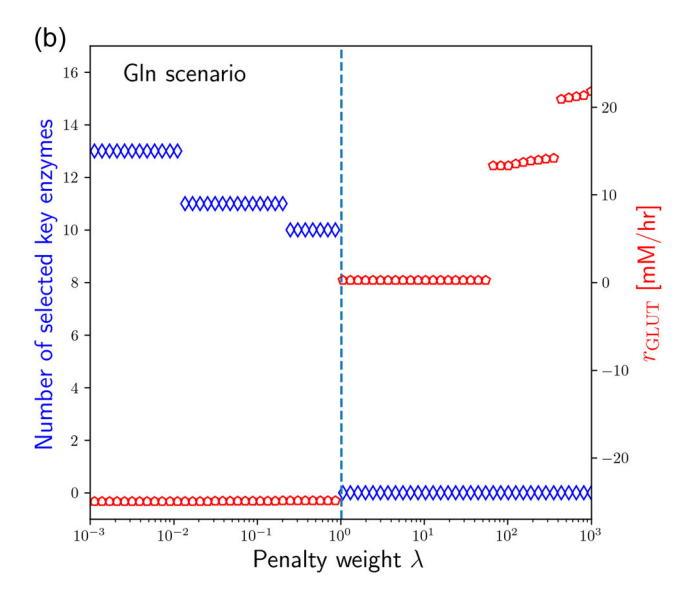


FIGURE 3 Selection of penalty weight λ value for key enzymes identification in Stage-1 SSO: (a) Optimal r_{GLUT} in each carbon source scenario for $\lambda \in [0.001,1000]$. The filled marker indicates the λ value used for key enzyme selection. (b) Number of selected key enzymes according to threshold δ and optimal r_{GLUT} in the Gln scenario within the same range of λ . The blue dashed line denotes the selected λ value representing the trade-off between the improvement in r_{GLUT} and minimization of numbers of enzyme adjustments.

to be altered in the SSO while fixing the abundance levels of all other enzymes at their original values. The optimal solutions of different enzyme combinations that show improvements in glucose production rate are shown in Figure 4. With up to five enzyme adjustments in \mathcal{R}^{stg1} , all scenarios reach the glucose production levels obtained through all-enzyme optimization (see Table 1). The Glyc scenario already produces a significant amount of glucose with the expression of GNG enzymes as well as the amplification in the entry enzyme, while the Gln scenario requires a larger number of enzyme interventions to produce glucose than the others.

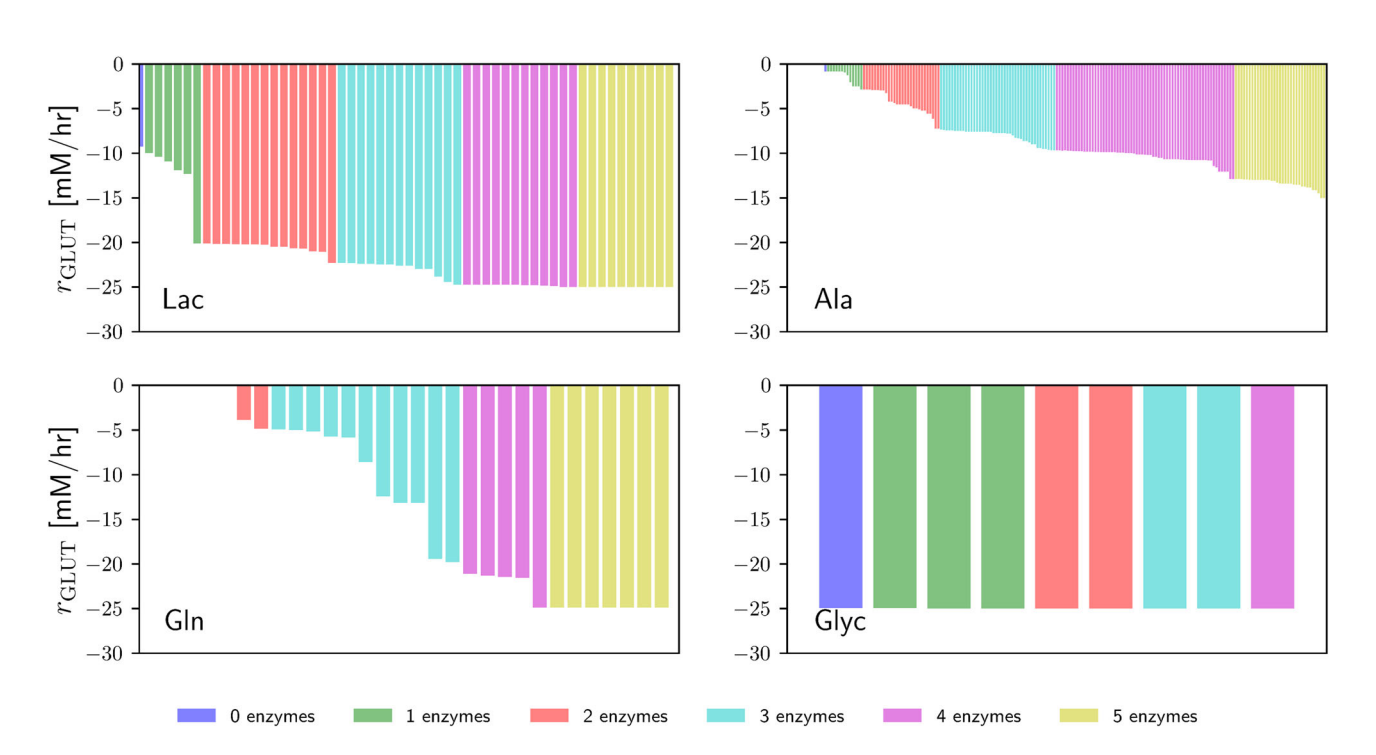
Metabolic requirements for gluconeogenesis

The optimal five-enzyme adjustments for the four carbon sources are listed in Table 2. Different enzyme changes are required for different carbon sources. As expected, glycerol only requires small changes, mainly to reduce the glycolysis flux in the three irreversible glycolytic reactions. Restricting glucose entry into glycolysis through downregulation of HK is common in the Lac, Ala, and Gln scenarios. For Lac and Ala, downregulation of CS to reduce the diversion of pyruvate into the TCA cycle is observed. Carbon from Gln and a portion of Ala enter the mitochondria through glutamate; hence, we see upregulation of the glutamate mitochondrial carrier, GluH. Aligned with the stage-1 SSO result, different requirements of changes in the TCA cycle are observed among the different carbon sources.

The resulting flux maps for the best 5-enzyme combinations are shown in Figure S4. The flux profiles for the four carbon source scenarios predicted by the model are consistent with physiological understanding. The main carbon flow in the Glyc scenario involves only the upper glycolysis pathway and requires no additional NADH. Only a small adjustment of enzyme abundance is seen. Both Lac and Ala enter gluconeogenesis through pyruvate nodes in the cytoplasm and mitochondria, and both rely on PEP export from mitochondria to provide carbon for gluconeogenesis. Gln is distinct from Lac and Ala by entering the mitochondria solely through Glu and entering the TCA cycle through aKG. In the Lac scenario, LDHA supplies NADH for the reversed reaction of glyceraldehyde 3-phosphate dehydrogenase (GAPDH). In the Ala and Gln scenarios, the reducing equivalents are exported from the mitochondria through malate phosphate mitochondrial antiporter (MalPi) and malate dehydrogenase 1 (MDH1). Export of malate to the cytoplasm also serves to supply carbon for PEP generation and eventually to glucose.

Case study 2: Optimal enzyme interventions considering all carbon sources

In case study 1, SSO was applied to identify optimal enzyme alteration that maximizes the glucose production rate for each of the four different carbon sources. The obtained optimal enzyme adjustments differ across the carbon source scenarios. In the second



Optimization of enzyme combinations in Stage-2 SSO: Optimal r_{GLUT} for different enzyme combinations with fixed numbers of allowed enzyme adjustments. Each column corresponds to one enzyme combination. Enzyme combinations are grouped based on the number of enzyme changes. Only the enzyme combinations that result in improvements in r_{GLUT} compared to the optimal solutions to fewer numbers of enzyme adjustments are kept. SSO, single-scenario optimization.

TABLE 2 Comparison of SSO and MSO Stage-2 optimization results with the number of enzyme adjustments set to five (n = 5)

Enzyme	e	HK1	HK2	CS	ME1	ME2	ACLY	GluH	SDH	AKGD	σ	PKM1	MalPi	CitMal
SSO	Lac	0.01	0.07	0.03	0.02		0.04							
	Ala	0.06		0.02	0.01	0.03		100						
	Gln			0.03				16.1	13.8	8.0	0.16			
	Glyc	0.21	0.58								0.1	0.64		
MSO		0.08						100			0.02		100	0.09

Abbreviations: MSO, multi-scenario optimization; SSO, single-scenario optimization.

case study, we focused on applying MSO to identify the optimal adjustment of a limited number of enzymes that simultaneously maximizes the glucose production rates from all carbon sources, as is more likely the case in bioprocess conditions.

3.2.1 | Stage-1 results

The value of λ is varied over a wider range (10⁻⁵ - 10³) in MSO to identify a suitable trade-off point for key enzyme selection, as shown in Figure S5a. All enzymes are allowed to change their abundance in the same range as in SSO. Same as in SSO, the glucose production rate increases with decreasing λ and eventually reaches a steady value. The significant increase in the reverse glycolysis flux in Gln appears at a much lower λ value compared to the other carbon sources, implying that glutamine has a higher metabolic barrier to overcome for gluconeogenesis. This result agrees with what we observed in the stage-2 result of SSO (see Figure 4). MSO can reach the same levels of glucose production as SSO for all carbon sources but at a lower λ value ($\lambda = 10^{-3}$). The optimal value of the convex penalty term, $P = \sum_{j \in \mathcal{R}} (log\alpha_j)^2$, is a measurement of the total amount of changes in enzyme abundance. Table 3 shows the results from SSO and MSO obtained using the same λ value. One can clearly see that to simultaneously meet the metabolic requirements of all carbon sources in MSO, the required total adjustments in enzyme abundance are much larger than what is needed if each carbon source is considered individually in SSO.

The largest λ value that reaches the maximum r_{GLUT} values in all scenarios is selected as the trade-off point for the identification of the key enzymes. The selected EM enzymes are shown in Figure S5b. The same trends of changes in the metabolic pathways as in SSO are observed. More enzymes are identified in MSO than in SSO. Almost every selected enzyme can be found in at least one of the four optimal enzyme sets identified in SSO, except for aspartate-glutamate mitochondrial transporter (AspGlu), citrate-malate mitochondrial transporter (CitMal), glutamic-oxaloacetic transaminase 2 (GOT2), and isocitrate dehydrogenase (IDH). Prominently upregulated are several mitochondrial transporters, while many glycolysis enzymes are downregulated. The newly identified enzymes in MSO are all linked to the TCA cycle. The differences can be attributed to the

TABLE 3 Comparison of SSO and MSO Stage-1 results at $\lambda = 10^{-3}$: optimal r_{GLUT} and values of the convex penalty term, $P = \sum_{j \in \mathscr{R}} (log\alpha_j)^2$, which represents the total amount of enzyme adjustments

Carbon-	source scen	ario	Lac	Ala	Gln	Glyc
SSO	r _{GLUT} [r	mM/h]	-25.0	-16.6	-25.0	-25.0
	P		16.6	25.2	13.9	9.7
MSO	r _{GLUT} [r	nM/h]	-25.0	-16.6	-25.0	-25.0
	Р		51.6			

Abbreviations: MSO, multi-scenario optimization; SSO, single-scenario optimization.

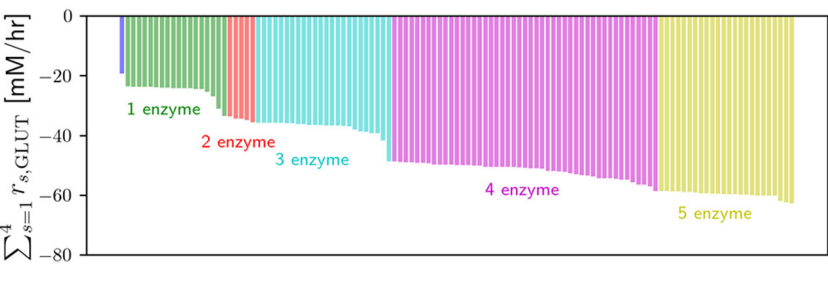
additional adjustments that are required to meet the different metabolic requirements of all carbon sources in the TCA cycle.

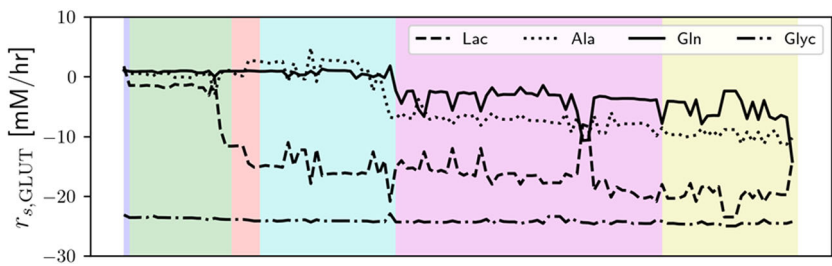
3.2.2 | Stage-2 results

As in SSO, GNG and carbon-entry enzymes are allowed to change their abundance in Stage-2 optimization. Combinations of up to five enzymes from the key enzyme set are generated and applied in MSO. The optimal r_{GLUT} for all four scenarios are shown in Figure 5. Again, glycerol requires only minimum changes to produce glucose. With an increasing number of enzyme adjustments, glucose production is gradually achieved in the other three carbon source scenarios. Upon allowing five enzymes to change their abundance levels, glucose can be produced at significant rates in all carbon source scenarios.

3.2.3 | Comparison of Stage-2 results from SSO and MSO

A key observation is that the maximum glucose production rates obtained from MSO are lower than the ones from SSO for a given number of allowed enzyme adjustments. This indicates that to effectively produce glucose from all carbon sources using the same set of altered enzymes, a compromise has to be found between the different scenarios. The MSO solution is the best compromise as





defined by its objective function but may not be individually optimal for a single carbon source.

The optimal five-enzyme interventions of MSO are listed in Table 2. We see downregulation of HK1 and σ to help reduce glycolysis flux, and upregulation of GluH to increase the carbon flux into the mitochondria in both MSO as well as the Ala and Gln scenarios of SSO. The other changes are related to cytoplasm-mitochondrion transport. Downregulation of CitMal prevents leakage of citrate into the cytoplasm and its generation of cytosolic acetyl-CoA, while overexpression of MalPi helps export mitochondrial Mal to supply cytosolic reducing equivalent and carbons. Note that high expressions of MalPi and GluH are also seen in liver and kidney (Gutiérrez-Aguilar & Baines, 2013: Monné et al., 2019). The metabolic flux profile for each carbon source resulting from the 5-enzyme intervention is similar to that seen in SSO (see Figure 6). In the Gln and Lac scenarios, the fluxes from both the MSO and SSO solutions all flow in the same direction. Some notable differences are seen in the Glyc scenario in that a small flux in the lower glycolysis pathway is seen in the MSO solution but not in the SSO solution, resulting in a small increase in fluxes across the mitochondrial membrane. In the Ala scenario, all fluxes maintain the same direction in MSO and SSO except that the PEP flux between the mitochondrion and the cytoplasm is reversed.

3.2.4 | Metabolic shift between glycolysis and gluconeogenesis

We next examine whether glycolysis is still permissible under a high glucose concentration (10 mM) upon the best 5-enzyme intervention obtained from MSO. To shift from a gluconeogenic state to a glycolytic state, the σ value has to be shifted to a high value (see Figure S6). The reversal of the direction of the glycolysis flux in the optimized five-enzyme intervention is accompanied by changes in metabolite concentrations. The relative concentrations, defined as the ratios between the concentrations in the optimized gluconeogenic state and those in the glycolytic state, are color-coded in

Figure 6. Here, $\,\sigma\,$ is set to 25 in the reference glycolytic state. The direction of change for shifting from the glycolytic state to the gluconeogenic state for all four substrates is very similar for the vast majority of metabolites. A striking difference among the carbon sources is in the trans-mitochondrial membrane traffic of metabolites involved in the reducing equivalent balance; while Lac generates a large quantity of reducing equivalent in the cytoplasm, Gln and Ala produce their reducing equivalent in the mitochondrion and export it to the cytoplasm through malate.

A major effector regulating the glycolytic and gluconeogenic states in liver is F26BP: high concentrations activate PFK and promote glycolysis, while low concentrations activate FBPase and favor gluconeogenesis (Okar et al., 2001; Wu et al., 2006). The F26BP level is modulated by σ , i.e. the relative level of kinase to phosphatase activity. The identification of a low σ as one of 5-enzyme adjustments to reverse the glycolysis flux and a high σ as the driver to revert to a glycolytic state is thus consistent with our physiological understanding. In liver, the adjustment of the σ value and switching of the flux state are mediated by the hormone glucagon through phosphorylation of PFKFB (Payne et al., 2005; Rider et al., 2004). Most cultured cells lack gluconeogenic enzymes and express different isoforms of PFKFB than in liver; nevertheless, they respond to environmental and physiological cues to modulate glycolytic flux via the σ value. For example, both signaling pathways AKT and AMPK regulate the σ value through posttranslational events (Liang & Mills, 2013; Ros & Schulze, 2013); a peptide TIGAR induced by P53 under stress conditions functions as fructose-2,6-bisphosphatase, thereby lowering glycolytic fluxes (Bensaad et al., 2006). To enable a cell line engineered as prescribed by the optimization results of MSO to switch between forward and reverse flux states, one may employ a biochemical inhibitor such as Chalcones, Phenoxyindoles, and Biarylsulfonamides to manipulate the σ value (Macut et al., 2019). Alternatively, one could use an inducible mutant PFKFB with only kinase or phosphatase activity to modulate the F26BP concentration.

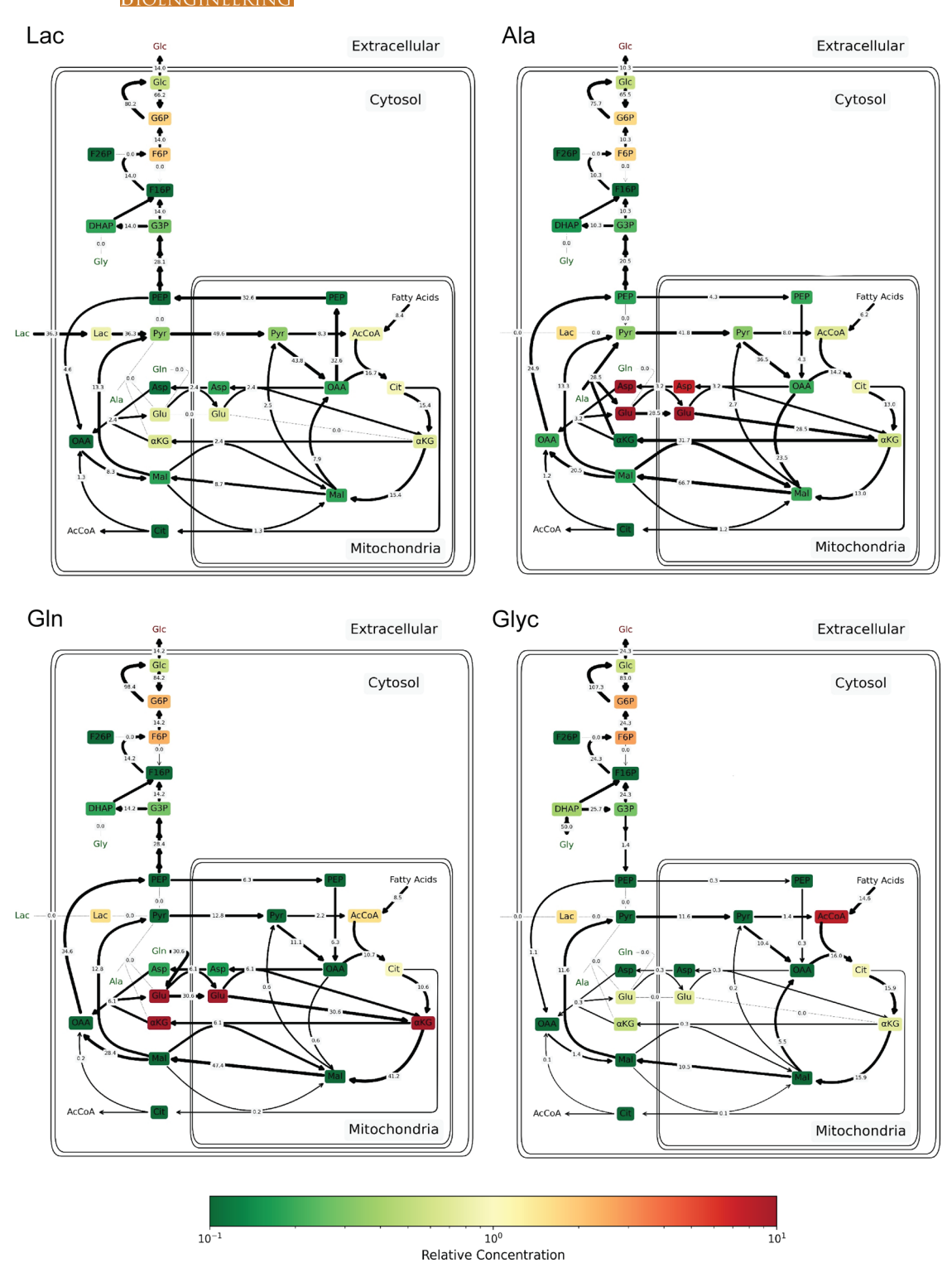


FIGURE 6 Flux and relative concentration maps associated with the optimal 5-enzyme MSO solution. The reference concentration profile is obtained with σ = 25 and 10 mM external glucose concentration. An increase in concentration is shown in red, while a decrease is shown in green. MSO, multi-scenario optimization.

4 | CONCLUSIONS

In this study, we developed a computational pathway optimization tool that employs a detailed kinetic metabolic model and a new twostage framework to find optimal multi-enzyme alterations that achieve a given metabolic objective. It also incorporates multiscenario optimization, which can be used to simultaneously target multiple physiological conditions. The optimization problem is formulated such that it allows gene insertion of nonnative reactions and up/downregulation. Using a convex penalty term, high-impact enzymes are identified in stage 1 of the proposed algorithm, which avoids the exhaustive search of enzyme combinations. These enzymes are then considered in stage 2, which determines the optimal interventions for specified numbers of enzyme adjustments. Moreover, by applying a state-of-the-art global optimization solver, we eliminated the need of trying a large number of initial guesses.

In the computational case studies, we applied the proposed method to reverse the glycolytic flux in cultured mammalian cells, which can avoid the need of glucose feed in the late culture stage and thereby improve process robustness. Two types of optimization problems, SSO and MSO, were implemented to study the metabolic requirements of reverse glycolysis from different carbon substrates. SSO determines the metabolic requirements for different carbon sources, which are mainly driven by the redox balance of NADH. MSO identifies one set of enzyme adjustments that simultaneously optimize the fluxes in multiple carbon scenarios. The MSO result aligns with the physiological understanding of reverse glycolysis; two mitochondrial transporters that show high expression in gluconeogenic tissues (MalPi and GluH) are suggested to be upregulated, and the kinase/phosphatase activity of PFKFB is recognized as the key control node for switching the metabolic states between glycolysis and gluconeogenesis.

The adoption of the kinetic metabolism model and multi-scenario optimization greatly enhances the versatility of pathway optimization; however, it also comes at the cost of significantly increased computational complexity. Due to the strong nonlinearity and the large size of the MSO problem, the solver was not able to find an initial feasible solution using its default multi-start search procedure. However, we found that providing the SSO solution as an initial guess reliably allowed the solver to find a starting feasible solution after which it was able to converge to the optimal solution. In other applications, a good physiological understanding of the targeted problem can often help the user devise similar initialization strategies. In this study, we included only the essential pathways in the kinetic model and considered only a small number of scenarios. One can expect the global solver to experience even more computational difficulties when more metabolic pathways and scenarios are included. To enable the solution of such large-scale pathway optimization problems in the future, we will explore the use of efficient decomposition methods, e.g. progressive hedging (Rockafellar & Wets, 1991) and Lagragean decomposition (Guignard & Kim, 1987).

While we have chosen the energy metabolism pathways as a model system in the computational case studies because they have been well studied and are hence well suited to assess the efficacy of our approach, it is important to note that the proposed optimization scheme has wider applicability. For example, glycosylation profiles of recombinant therapeutic proteins may vary in the different stages of culture, affecting product quality (Sumit et al., 2019). Kinetic-model-based pathway engineering has been attempted for modulating the glycosylation profile (Stach et al., 2019). Our proposed multi-scenario optimization approach may further facilitate pathway engineering for optimizing glycosylation profiles under different process conditions.

In drug discovery, the physiological ramifications of a disorder in a metabolic network may vary under different conditions for a patient. Also here, multi-scenario optimization could help devise drug regimens for multiple conditions. In general, the proposed optimization framework is an efficient and versatile tool that can be used to guide metabolic engineering strategies as well as test metabolic hypotheses in complex cellular systems.

AUTHOR CONTRIBUTIONS

Yen-An Lu: Conceptualization, methodology, software, case studies, writing-original draft. Conor O'Brien: Conceptualization, methodology, software, case studies. Douglas Mashek: Writing-review and editing. Wei-Shou Hu: Conceptualization, methodology, supervision, writing-review and editing, funding acquisition. Qi Zhang: Conceptualization, methodology, supervision, writing-review and editing, funding acquisition.

ACKNOWLEDGMENTS

The authors gratefully acknowledge the support from the National Science Foundation under Grant #2044077. Computational resources were provided by the Minnesota Supercomputing Institute at the University of Minnesota.

CONFLICTS OF INTEREST

The authors declare no conflicts of interest.

ORCID

Qi Zhang http://orcid.org/0000-0001-8862-4675

REFERENCES

Andreas, W., & Lorenz, T. B. (2006). On the implementation of an interiorpoint filter line-search algorithm for large-scale nonlinear programming. *Mathematical Programming*, 25–57.

Bensaad, K., Tsuruta, A., Selak, M. A., Vidal, M. N. C., Nakano, K., Bartrons, R., Gottlieb, E., & Vousden, K. H. (2006). TIGAR, a p53-inducible regulator of glycolysis and apoptosis. *Cell*, 126, 107–120. https://doi.org/10.1016/j.cell.2006.05.036

Berndt, N., Bulik, S., Wallach, I., Wünsch, T., König, M., Stockmann, M., Meierhofer, D., & Holzhütter, H. G. (2018). HEPATOKIN1 is a biochemistry-based model of liver metabolism for applications in medicine and pharmacology. *Nature Communications*, *9*, 2386. https://doi.org/10.1038/s41467-018-04720-9

Buchsteiner, M., Quek, L. E., Gray, P., & Nielsen, L. K. (2018). Improving culture performance and antibody production in CHO cell culture processes by reducing the Warburg effect. *Biotechnology and Bioengineering*, 115, 2315–2327. https://doi.org/10.1002/bit.26724

Burgard, A. P., & Maranas, C. D. (2003). Optimization-based framework for inferring and testing hypothesized metabolic objective functions. *Biotechnology and Bioengineering*, 82, 670–677. https://doi.org/10. 1002/bit.10617

Chae, T. U., Choi, S. Y., Kim, J. W., Ko, Y. S., & Lee, S. Y. (2017). Recent advances in systems metabolic engineering tools and strategies. *Current Opinion in Biotechnology*, 47, 67–82. https://doi.org/10.1016/j.copbio.2017.06.007

Charaniya, S., Le, H., Rangwala, H., Mills, K., Johnson, K., Karypis, G., & Hu, W. S. (2010). Mining manufacturing data for discovery of high productivity process characteristics. *Journal of Biotechnology*, 147, 186–197. https://doi.org/10.1016/j.jbiotec.2010.04.005



- Chowdhury, A., Zomorrodi, A. R., & Maranas, C. D. (2014). k-OptForce: Integrating kinetics with flux balance analysis for strain design. *PLoS Computational Biology*, 10, e1003487. https://doi.org/10.1371/journal.pcbi.1003487
- Edwards, J. S., & Palsson, B. O. (2000). The *Escherichia coli* MG1655 in silico metabolic genotype: its definition, characteristics, and capabilities. *Proceedings of the National Academy of Sciences*, 97, 5528–5533. https://doi.org/10.1073/pnas.97.10.5528
- Foster, C. J., Wang, L., Dinh, H. V., Suthers, P. F., & Maranas, C. D. (2021). Building kinetic models for metabolic engineering. *Current Opinion in Biotechnology*, 67, 35–41. https://doi.org/10.1016/j.copbio.2020. 11.010
- Gagnon, M., Hiller, G., Luan, Y. T., Kittredge, A., Defelice, J., & Drapeau, D. (2011). High-end pH-controlled delivery of glucose effectively suppresses lactate accumulation in CHO fed-batch cultures. Biotechnology and Bioengineering, 108, 1328–1337. https://doi.org/10.1002/bit.23072
- Guignard, M., & Kim, S. (1987). Lagrangean decomposition: A model yielding stronger lagrangean bounds. *Mathematical Programming*, 39, 215–228. https://doi.org/10.1007/BF02592954
- Gutiérrez-Aguilar, M., & Baines, C. P. (2013). Physiological and pathological roles of mitochondrial SLC25 carriers. *Biochemical Journal*, 454, 371–386. https://doi.org/10.1042/BJ20121753
- Hart, W. E., Laird, C., Watson, J. -P., & Woodruff, D. L. (2017). Pyomo Optimization modeling in Python (2nd ed.). Springer. http://link. springer.com/10.1007/978-1-4614-3226-5
- Hassell, T., Gleave, S., & Butler, M. (1991). Growth inhibition in animal cell culture - The effect of lactate and ammonia. Applied Biochemistry and Biotechnology, 30, 29–41. https://doi.org/10.1007/BF02922022
- Hatzimanikatis, V., Floudas, C. A., & Bailey, J. E. (1996). Analysis and design of metabolic reaction networks via mixed-integer linear optimization. AIChE Journal, 42, 1277–1292. https://doi.org/10. 1002/aic.690420509
- Huccetogullari, D., Luo, Z. W., & Lee, S. Y. (2019). Metabolic engineering of microorganisms for production of aromatic compounds. *Microbial Cell Factories*, 18, 41. https://doi.org/10.1186/s12934-019-1090-4
- Kacser, H., Burns, J. A., Kacser, H., & Fell, D. A. (1995). The control of flux. Biochemical Society Transactions, 23, 341–366. https://doi.org/10. 1042/bst0230341
- Kim, J., Reed, J. L., & Maravelias, C. T. (2011). Large-scale bi-level strain design approaches and mixed-integer programming solution techniques. PLoS One, 6, e24162. https://doi.org/10.1371/journal.pone. 0024162
- König, M., Bulik, S., & Holzhütter, H. G. (2012). Quantifying the contribution of the liver to glucose homeostasis: A detailed kinetic model of human hepatic glucose metabolism. *PLoS Computational Biology*, 8, e1002577. https://doi.org/10.1371/journal.pcbi. 1002577
- Lao, M. S., & Toth, D. (1997). Effects of ammonium and lactate on growth and metabolism of a recombinant Chinese hamster ovary cell culture. *Biotechnology Progress*, 13, 688-691. https://doi.org/10. 1021/bp9602360
- Lian, J., Mishra, S., & Zhao, H. (2018). Recent advances in metabolic engineering of *Saccharomyces cerevisiae*: New tools and their applications. *Metabolic Engineering*, 50, 85–108. https://doi.org/10. 1016/j.ymben.2018.04.011
- Liang, J., & Mills, G. B. (2013). AMPK: A contextual oncogene or tumor suppressor. Cancer Research, 73, 2929–2935. https://doi.org/10. 1158/0008-5472.CAN-12-3876
- Lin, P. C., Saha, R., Zhang, F., & Pakrasi, H. B. (2017). Metabolic engineering of the pentose phosphate pathway for enhanced limonene production in the cyanobacterium *Synechocystis* sp. PCC. *Scientific Reports*, 7, 17503. https://doi.org/10.1038/s41598-017-17831-y

- Liu, Y., & Nielsen, J. (2019). Recent trends in metabolic engineering of microbial chemical factories. Current Opinion in Biotechnology, 60, 188-197. https://doi.org/10.1016/j.copbio.2019.05.010
- Lucidi, S., & Rinaldi, F. (2010). Exact penalty functions for nonlinear integer programming problems. *Journal of Optimization Theory and Applications*, 145, 479-488. https://doi.org/10.1007/s10957-010-9700-7
- Lucidi, S., & Rinaldi, F. (2013). An exact penalty global optimization approach for mixed-integer programming problems. *Optimization Letters*, 7, 297–307. https://doi.org/10.1007/s11590-011-0417-9
- Machado, D., & Herrgård, M. J. (2015). Co-evolution of strain design methods based on flux balance and elementary mode analysis. *Metabolic Engineering Communications*, 2, 85–92. https://doi.org/10. 1016/j.meteno.2015.04.001
- Macut, H., Hu, X., Tarantino, D., Gilardoni, E., Clerici, F., Regazzoni, L., Contini, A., Pellegrino, S., & Luisa Gelmi, M. (2019). Tuning PFKFB3 bisphosphatase activity through allosteric interference. *Scientific Reports*, 9, 20333. https://doi.org/10.1038/s41598-019-56708-0
- Monk, J. M., Lloyd, C. J., Brunk, E., Mih, N., Sastry, A., King, Z., Takeuchi, R., Nomura, W., Zhang, Z., Mori, H., Feist, A. M., & Palsson, B. O. (2017). iML1515, a knowledgebase that computes *Escherichia coli* traits. *Nature Biotechnology*, 35, 904–908. https://doi.org/10.1038/nbt.3956
- Monné, M., Vozza, A., Lasorsa, F. M., Porcelli, V., & Palmieri, F. (2019). Mitochondrial carriers for aspartate, glutamate and other amino acids: A review. *International Journal of Molecular Sciences*, 20, 4456. https://doi.org/10.3390/ijms20184456
- Moreno-Sánchez, R., Saavedra, E., Rodríguez-Enríquez, S., & Olín-Sandoval, V. (2008). Metabolic control analysis: A tool for designing strategies to manipulate metabolic pathways. *Journal of Biomedicine and Biotechnology*, 2008, 1–30. https://doi.org/10.1155/2008/597913
- Mulukutla, B. C., Gramer, M., & Hu, W. S. (2012). On metabolic shift to lactate consumption in fed-batch culture of mammalian cells. *Metabolic Engineering*, 14, 138–149. https://doi.org/10.1016/j. ymben.2011.12.006
- Mulukutla, B. C., Khan, S., Lange, A., & Hu, W. -S. (2010). Glucose metabolism in mammalian cell culture: New insights for tweaking vintage pathways. *Trends in Biotechnology*, 28, 476–484. https://doi. org/10.1016/j.tibtech.2010.06.005
- Mulukutla, B. C., Yongky, A., Daoutidis, P., & Hu, W. S. (2014). Bistability in glycolysis pathway as a physiological switch in energy metabolism. PLoS One, 9, e98756. https://doi.org/10.1371/journal.pone. 0098756
- Mulukutla, B. C., Yongky, A., Grimm, S., Daoutidis, P., & Hu, W. S. (2015).
 Multiplicity of steady states in glycolysis and shift of metabolic state in cultured mammalian cells. PLoS One, 10, e0121561. https://doi.org/10.1371/journal.pone.0121561
- Nikolaev, E. V. (2010). The elucidation of metabolic pathways and their improvements using stable optimization of large-scale kinetic models of cellular systems. *Metabolic Engineering*, 12, 26–38. https://doi.org/10.1016/j.ymben.2009.08.010
- O'Brien, C., Allman, A., Daoutidis, P., & Hu, W-SS. (2019). Kinetic model optimization and its application to mitigating the Warburg effect through multiple enzyme alterations. *Metabolic Engineering*, *56*, 154–164. https://doi.org/10.1016/j.ymben.2019.08.005
- Okar, D. A., Lange, A. J., Manzano, À., Navarro-Sabatè, A., Riera, L., & Bartrons, R. (2001). PFK-2/FBPase-2: Maker and breaker of the essential biofactor fructose-2,6-bisphosphate. *Trends in Biochemical Sciences*, 26, 30–35. https://doi.org/10.1016/S0968-0004(00) 01699-6
- Payne, V. A., Arden, C., Wu, C., Lange, A. J., & Agius, L. (2005). Dual role of phosphofructokinase-2/fructose bisphosphatase-2 in regulating the compartmentation and expression of glucokinase in hepatocytes.

- Diabetes, 54, 1949–1957. https://doi.org/10.2337/diabetes.54. 7 1949
- Pharkya, P., Burgard, A. P., & Maranas, C. D. (2004). OptStrain: A computational framework for redesign of microbial production systems. *Genome Research*, 14, 2367–2376. https://doi.org/10.1101/gr.2872004
- Polisetty, P. K., Gatzke, E. P., & Voit, E. O. (2008). Yield optimization of regulated metabolic systems using deterministic branch-and-reduce methods. *Biotechnology and Bioengineering*, 99, 1154–1169. https://doi.org/10.1002/bit.21679
- Richelle, A., & Lewis, N. E. (2017). Improvements in protein production in mammalian cells from targeted metabolic engineering. *Current Opinion in Systems Biology*, 6, 1–6. https://doi.org/10.1016/j.coisb. 2017.05.019
- Rider, M. H., Bertrand, L., Vertommen, D., Michels, P. A., Rousseau, G. G., & Hue, L. (2004). 6-Phosphofructo-2-kinase/fructose-2,6-bisphosphatase: Head-to-head with a bifunctional enzyme that controls glycolysis. *Biochemical Journal*, 381, 561–579. https://doi.org/10.1042/BJ20040752
- Rockafellar, R. T., & Wets, R. J. -B. (1991). Scenarios and policy aggregation in optimization under uncertainty. *Mathematics of Operations Research*, 16, 119–147. https://doi.org/10.1287/moor. 16.1.119
- Ros, S., & Schulze, A. (2013). Balancing glycolytic flux: the role of 6-phosphofructo-2-kinase/fructose 2,6-bisphosphatases in cancer metabolism. Cancer & Metabolism, 1, 8. https://doi.org/10.1186/2049-3002-1-8
- Sahinidis, N. V. (1996). BARON: A general purpose global optimization software package. *Journal of Global Optimization*, 8, 201–205. https://doi.org/10.1007/bf00138693
- Shen, F., Sun, R., Yao, J., Li, J., Liu, Q., Price, N. D., Liu, C., & Wang, Z. (2019). Optram: In-silico strain design via integrative regulatory-metabolic network modeling. PLoS Computational Biology, 15, e1006835. https://doi.org/10.1371/journal.pcbi.1006835
- Stach, C. S., McCann, M. G., O'Brien, C. M., Le, T. S., Somia, N., Chen, X., Lee, K., Fu, H. Y., Daoutidis, P., Zhao, L., Hu, W. S., & Smanski, M. (2019). Model-driven engineering of N-linked glycosylation in Chinese Hamster ovary cells. ACS Synthetic Biology, 8, 2524–2535. https://doi.org/10.1021/acssynbio.9b00215
- Sumit, M., Dolatshahi, S., Chu, A. H. A., Cote, K., Scarcelli, J. J., Marshall, J. K., Cornell, R. J., Weiss, R., Lauffenburger, D. A., Mulukutla, B. C., & Figueroa, B. (2019). Dissecting N-glycosylation dynamics in Chinese hamster ovary cells fed-batch cultures using time course omics analyses. *iScience*, 12, 102–120. https://doi.org/ 10.1016/j.isci.2019.01.006
- Templeton, N., & Young, J. D. (2018). Biochemical and metabolic engineering approaches to enhance production of therapeutic proteins in animal cell cultures. *Biochemical Engineering Journal*, 136, 40–50. https://doi.org/10.1016/j.bej.2018.04.008

- Vera, J., González-Alcón, C., Marín-Sanguino, A., & Torres, N. (2010).
 Optimization of biochemical systems through mathematical programming: Methods and applications. Computers & Operations Research, 37, 1427-1438. https://doi.org/10.1016/j.cor.2009.02.021
- Villaverde, A. F., Bongard, S., Mauch, K., Balsa-Canto, E., & Banga, J. R. (2016). Metabolic engineering with multi-objective optimization of kinetic models. *Journal of Biotechnology*, 222, 1–8. https://doi.org/ 10.1016/j.jbiotec.2016.01.005
- Vital-lopez, F. G., Armaou, A., Nikolaev, E. V., & Maranas, C. D. (2006). A computational procedure for optimal engineering interventions using kinetic models of metabolism. *Biotechnology Progress*, 22, 1507–1517.
- Wu, C., Khan, S. A., Peng, L. J., & Lange, A. J. (2006). Roles for fructose-2,6-bisphosphate in the control of fuel metabolism: beyond its allosteric effects on glycolytic and gluconeogenic enzymes. Advances in Enzyme Regulation, 46, 72–88. https://doi.org/10.1016/j. advenzreg.2006.01.010
- Wu, C., Okar, D. A., Newgard, C. B., & Lange, A. J. (2001). Overexpression of 6-phosphofructo-2-kinase/fructose-2,6-bisphosphatase in mouse liver lowers blood glucose by suppressing hepatic glucose production. *Journal of Clinical Investigation*, 107, 91–98. https://doi.org/10. 1172/JCI11103
- Yim, H., Haselbeck, R., Niu, W., Pujol-Baxley, C., Burgard, A., Boldt, J., Khandurina, J., Trawick, J. D., Osterhout, R. E., Stephen, R., Estadilla, J., Teisan, S., Schreyer, H. B., Andrae, S., Yang, T. H., Lee, S. Y., Burk, M. J., & Van Dien, S. (2011). Metabolic engineering of *Escherichia coli* for direct production of 1,4-butanediol. *Nature Chemical Biology*, 7, 445–452. https://doi.org/10.1038/nchembio.580
- Zomorrodi, A. R., Suthers, P. F., Ranganathan, S., & Maranas, C. D. (2012).

 Mathematical optimization applications in metabolic networks.

 Metabolic Engineering, 14, 672–686. https://doi.org/10.1016/j.

 ymben.2012.09.005

SUPPORTING INFORMATION

Additional supporting information can be found online in the Supporting Information section at the end of this article.

How to cite this article: Lu, Y.-A., Brien, C. M. O., Mashek, D. G., Hu, W.-S., & Zhang, Q. (2023). Kinetic-model-based pathway optimization with application to reverse glycolysis in mammalian cells. *Biotechnology and Bioengineering*, 120, 216–229. https://doi.org/10.1002/bit.28249